JOURNAL OF PROPULSION AND POWER
Vol. 20, No. 2, March–April 2004

Indium Field Emission Electric Propulsion Microthruster Experimental Characterization

M. Tajmar,* A. Genovese,† and W. Steiger‡
ARC Seibersdorf Research, A-2444 Vienna, Austria

Indium liquid metal ion sources have been flying for more than 10 years on a variety of spacecraft for spacecraft potential control and as the core element of mass spectrometers. Since 1995, a dedicated indium field emission electric propulsion (In-FEEP) thruster has been under development and recently passed a 2000-h endurance test. The In-FEEP thruster is a micropropulsion device for the 1–100 μN thrust range with low thrust noise and high resolution. The latest performance characteristics including direct thrust measurements and beam profiles are summarized. This information is very important for many upcoming missions that require ultraprecise drag-free control such as the Gravity Field and Steady-State Ocean Circulation Mission, LISA, Terrestrial Planet Finder/Darwin, or SMART-2.

Nomenclature

c	=	thrust coefficient factor, %
e	=	elementary charge, 1.6×10^{-19} C
F	=	force, N
g	=	standard gravitational acceleration, $9.81\ \mathrm{m \cdot s^{-2}}$
I_B, I_E, I_{extr}, I_{PS}	=	ion beam, emitter, extractor, plume shield current, A
I_{sp}	=	specific impulse, s
m_{ion}	=	indium ion mass, 1.906×10^{-25} kg
m_R	=	reservoir mass, kg
$\dot{m}_{\mathrm{ion}}$, $\dot{m}_{\mathrm{droplet}}$, $\dot{m}$	=	ion, droplet, total mass flow rate, $\mathrm{kg \cdot s^{-1}}$
r	=	emitter–accelerator distance, m
U_B, U_E	=	extractor bias, emitter voltage, V
v	=	velocity, $\mathrm{m \cdot s^{-1}}$
η_m	=	mass efficiency, %
τ	=	temperature, K

Introduction

FIELD emission thrusters are currently considered for a large variety of space missions both in the Unites States and in Europe. They offer low thrust noise and high controllability combined with a very high specific impulse (up to 8000 s) enabling ultra-high-precision pointing capabilities. Such thrusters are required for scientific drag-free and constellation missions such as LISA, Terrestrial Planet Finder Darwin, Gravity Field and Steady-State Ocean Circulation Mission (GOCE), and SMART-2.

A dedicated indium field emission electric propulsion (In-FEEP) thruster based on space-proven miniaturized indium liquid-metal-ion-sources (LMIS)[1–5] has been under development since 1995. Developed more than 20 years ago, indium LMIS were first successfully tested onboard of the Russian MIR space station in 1991 and have since flown on a number of satellites as part of a spacecraft potential control and mass spectrometer device (see Table 1). This makes it the only space-proven LMIS logging more than 2700 h of combined operation in space. They have also demonstrated excellent robustness, surviving an Ariane 5 launch failure onboard the Cluster satellite. After retrieval from the swamps, ion emission was started with characteristics similar to previous ground testing.[2]

Significant research was concentrated on scaling the ion emission from a few micronewtons of thrust (corresponding to typical current levels for the aforementioned space instruments) to the 100-μN thrust range. This includes emission optimization at high currents, addressing lifetime degradation issues, and the development of larger propellant reservoirs and thruster module housings. The paper describes the current status of the In-FEEP thruster technology and summarizes all major performance data that have been obtained.

Thruster Description

The thruster core consists of an In-LMIS producing an energetic indium ion beam that creates thrust. Indium was chosen as a propellant due its high atomic mass, low ionization potential, and good wetting properties. Moreover, it can be handled in atmosphere with no risk, contrary to alkali metals such as cesium or gallium, which are also used for FEEP thrusters.[6] This greatly simplifies testing and also relaxes complex sealing procedures before launch. Tradeoffs between the different FEEP propellants may be found in Ref. 7.

The ion source consists either of a needle covered with indium or a capillary with indium inside, which is heated above the indium melting point (156.6°C). Then a sufficiently high electric potential is applied between the emitter and an extractor electrode until a field strength of about 10^9 V/m is reached at the tip. The equilibrium between the surface tension and the electric field strength forms a so-called Taylor cone on the surface (see Ref. 8) with a jet protruding due to space charge (Fig. 1). Atoms are then ionized at the tip of the jet and accelerated out by the same field that created them. The expelled ions are replenished by the hydrodynamic flow of the liquid metal. Contrary to other electric propulsion systems, ionization and acceleration takes place in one step using the same electric field. This leads to a very high electric efficiency of >95%, as we will show in a later section of this paper. Indium ions are 98% singly charged along the complete thrust range.[3]

Depending on the total impulse that the thruster has to deliver, several different tank reservoirs were developed ranging from 0.22 up to 30 g of indium capacity (Fig. 2). The indium flow toward the emission site is enhanced by capillary forces using fins inside the reservoir structure. The reservoir tank is typically mounted within a thermal isolator, which also contains heaters to liquefy the propellant (Fig. 3).

In addition to charged ions, slightly charged microdroplets are emitted from the emission site. They have a typical diameter of 0.1 μm and a mass of 1.91×10^{-18} kg. According to Thompson and von Engel,[9] there is a lower limit of the mass-to-charge ratio

Received 18 July 2002; revision received 18 December 2002; accepted for publication 26 September 2003.

*Staff Member, Space Propulsion; also Lecturer, Aerospace Engineering Department, Vienna University of Technology, A-1040 Vienna, Austria; martin.tajmar@arcs.ac.at. Member AIAA.
†Staff Member, Space Propulsion; angelo.genovese@arcs.ac.at.
‡Senior Staff Member, Space Propulsion; wolfgang.steiger@arcs.ac.at.

Table 1 Space experience of ARCS indium LMIS (up to February 2002)

Experiment	Function	Spacecraft	Number of LMIS	Operation time
LOGION	Test of LMIS in microgravity	MIR	1	24 h (1991)
MIGMAS/A	Mass spectrometer	MIR	1	120 h (1991–1994)
EFE-IE	Spacecraft potential control	GEOTAIL	8	600 h (1992–)
PCD	Spacecraft potential control	EQUATOR-S	8	250 h (1998)
ASPOC	Spacecraft potential control	Cluster	32	Ariane 5 launch failure 1996 still operational after crash
ASPOC-II	Spacecraft potential control	Cluster-2	32	1715 h (2000–)
COSIMA	Mass spectrometer	ROSETTA	2	To be launched 2003
ASPOC/DSP	Spacecraft potential control	DoubleStar	4	To be launched 2004

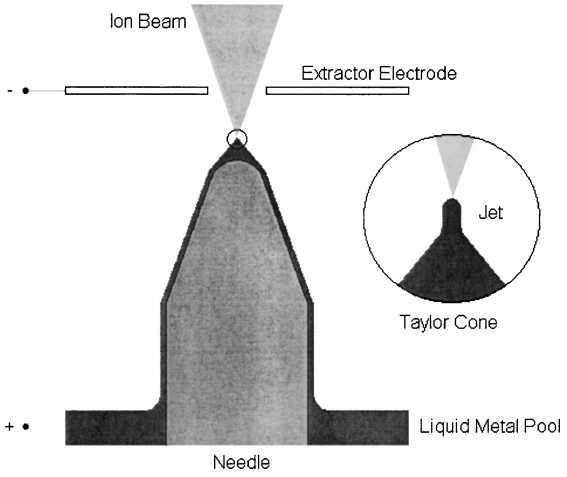

Fig. 1 In-FEEP thruster principle.

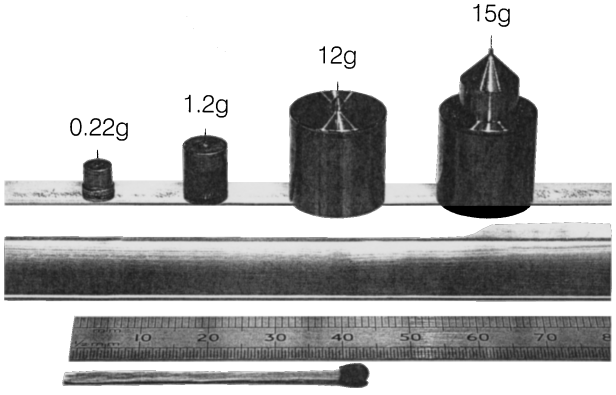

Fig. 2 Indium LMIS with different indium reservoir sizes.

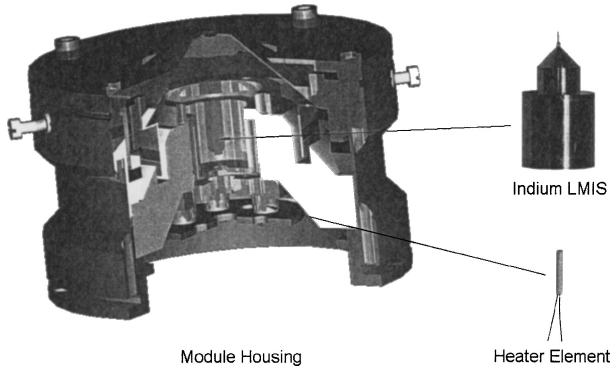

Fig. 3 In-FEEP thruster consisting of indium LMIS, heater element, and module housing.

for a stable droplet. Below this limit, the droplet gets distorted by developing Taylor cones leading to field evaporation of the droplet. When a magnetic deflection technique was used, the lower limit for the mass-to-charge ratio was found to be 6.26×10^{-2} kg/C. This limit together with the measured mass of the droplets leads to an upper limit of 191 elementary charges on each droplet. A lengthy discussion on droplet properties and measurements may be found in Ref. 10. Those droplets can contaminate the extractor electrode closing the hole in front of the emitter. To evaporate the indium contamination to reduce this lifetime risk, a heatable extractor ring can be used instead of an extractor plate. This extractor ring requires an additional power supply and adds another lifetime risk, which is the sputtering of the ring from beam ions. However, the heatable extractor is necessary for a lifetime of >5000 h. The evaporation requires a power of about 5 W and lasts 1 min to remove all indium from the extractor. This procedure has to be carried out every 200 h to maintain low contamination (indium thickness on wire to be smaller than 0.4 mm) and fast evaporation. Spacecraft contamination from microdroplets and charge-exchange ions was numerically modeled[11] showing that it is negligible. Moreover, a dedicated contamination test is presently running as part of an extended In-FEEP endurance test.[12]

Typical emitter voltages range from $U_E = 5$ to 10 kV for currents of $I_E = 10$–$600\ \mu$A. This corresponds to a thrust of 1–64 μN. To avoid backstreaming of ambient plasma electrons toward the ion emitter (depending on the plasma density in the respective satellite orbit), the extractor ring or a plume shield above the extractor can be biased negative with respect to ground. This configuration is shown in Fig. 4. It has been observed that a bias voltage of $U_B = -1$ kV is sufficient to eliminate any electron backstreaming into the emitter even for high ambient plasma densities, such as low Earth orbit. The following equations determine the thruster performance with respect to thrust force F and specific impulse I_{sp}:

$$F = \dot{m}_{ion} \cdot v = (I_E - I_{extr} - I_{PS}) \cdot \sqrt{2 \cdot m_{ion} \cdot U_E / e} \cdot c(I_E)$$

$$= 1.543 \times 10^{-3} \cdot I_B \cdot \sqrt{U_E} \cdot c(I_E) \quad (1)$$

$$I_{sp} = F/\dot{m} \cdot g = 132.1 \cdot \sqrt{U_E} \cdot c(I_E) \cdot \eta_m(I_E) \quad (2)$$

Thrust losses due to beam divergence, described by the thrust coefficient factor $c(I_E)$, are usually $20 \pm 10\%$ (depending on the actual configuration and thrust level), which is in agreement with direct thrust and plume measurements.[13–15] Use of a thermionic neotralizer is assumed in the calculation. By expressing the current integral as a function of the reservoir size, we can also express the thrust integral (neglecting extractor and plume shield currents):

$$\int I_E \cdot \frac{m_{ion}}{e} \cdot \mathrm{d}t = m_R \cdot \eta_m(I_E) \quad (3)$$

$$\int F \cdot \mathrm{d}t \cong 1.543 \times 10^{-3} \cdot \frac{e}{m_{ion}} \cdot \sqrt{U_E} \cdot c(I_E) \cdot m_R \cdot \eta_m(I_E)$$

$$= 1299.4 \cdot \sqrt{U_E} \cdot c(I_E) \cdot m_R \cdot \eta_m(I_E)$$

Plume measurements as well as modeling showed that space charge potentials are very low for In-FEEP thrusters[16,17] and that

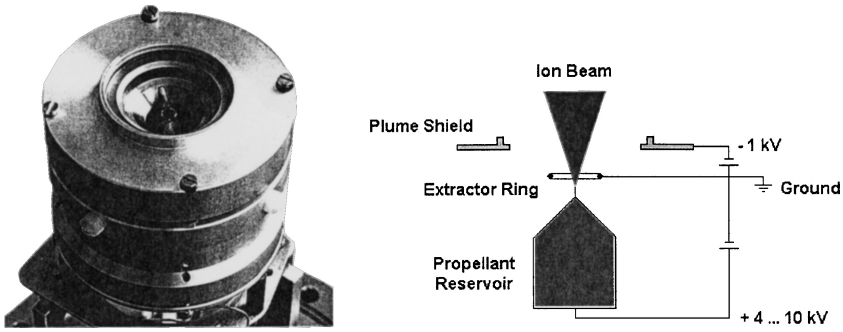

Fig. 4 In-FEEP with a) extractor heater configuration and b) electric configuration.

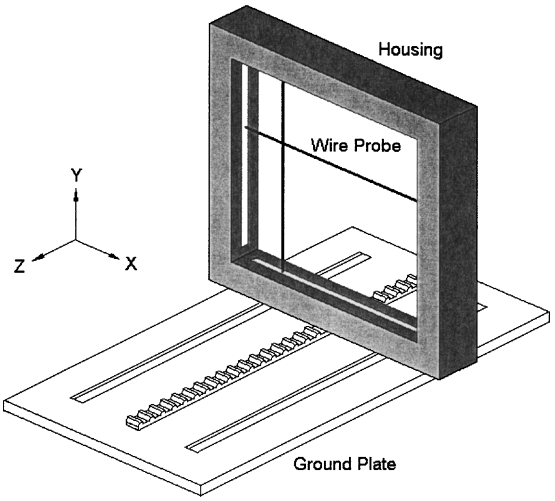

Fig. 5 Beam diagnostics setup.

no potential humps form inside the ion beam that would case the beam to stall. Therefore, a neutralizer is only needed to maintain the spacecraft floating potential, not to neutralize the ion beam itself.

Performance Characteristics

Beam Diagnostics

The ion beam distribution was measured using wire probes that can move either in X or Y direction (Fig. 5). The probes consist of a 1.6-mm-diam tungsten wire, which is biased to -28 V to repel secondary electrons from the facility or the probe itself. They are moved using Phytron stepper motors (Model VSS-HV 42.200.2.5), which are high-vacuum compatible. The whole probe assembly can be moved in the thrust direction on a ground plate using a larger Phytron VSS-HV 52.200.5.0 stepper motor. All stepper motors are controlled using a custom LabView program, a National Instruments PCI-7334 stepper motion controller, and Phytron ZSO 42-40 and ZSO 72-70 power stages. The probe current measurements are done using Keithley 485 picoamperemeters, and the output was connected again to the LabView program using a National Instruments PCI-6036E data acquisition card and an AI-03 isolation amplifier. Each current measurement was averaged over 100 samples; the accuracy was always $<1\%$ of the measured value.

In a first step, only one wire probe was used to test and verify the whole set-up and LabView program. However, one-dimensional data were also used for a good thruster characterization. Because we use only rotationally symmetric electrodes, the ion beam must be rotationally symmetric as well. This is also indicated by the low extractor currents (usually around 1% of the emitter current). Using this symmetry, we can calculate the real beam ion density using a reconstruction algorithm used, for example, in medical computer tomography. The algorithm, as well as verification of the calculations, may be found in Ref. 18. This ion beam density allows us to compute the precise thrust correction coefficient c from electrical measurements only.

Figure 6 shows the beam profiles from the Y-wire probe at a distance of 30 mm from the thruster's needle tip at beam currents from 10–600 μA. All measurements were done in a vacuum chamber with a diameter of 0.8 m and a length of 1.2 m at a pressure of about 10^{-6} mbar (varying with thrust range due to outgassing of the collector from ion beam bombardment). The positioning accuracy is better than 0.5 mm; hence, the angle accuracy was better than 1 deg. All beam profiles were done using a 15-g indium LMIS in a configuration similar to Fig. 4 with the plume shield biased at -1 kV (extractor diameter 4 mm, emitter–extractor distance 0.2 mm). The initial half-angle beam divergence at 10 μA is about 28 deg. Up to 400 μA, the ion beam is well within the 60-deg half-angle limit from the plume shield. Then the geometrical limit influences significantly the beam shape. At currents below 400 μA, the beam shape resembles a near-Gaussian bell shape, after 400 μA, the geometrical limits reshapes the beam more closely to a near-cosine distribution. Even at maximum current, the ion beam does not go beyond 60 deg. (The slightly larger value in the Fig. 6 is due to the diameter of the probe.)

The total ion beam divergence for each beam current is shown in Fig. 7. The steep increase in beam divergence at low currents indicates that beam divergence is initially dominated by the ion beam's space charge. From 100 μA, the geometrical limitation from the plume shield takes over as the dominant factor. This curve is similar to the one derived from old measurements.[15]

Figure 8 shows the computed thrust coefficient factor c along the beam current ranging from 0.91 at low currents to 0.76 at 600 μA. The values are slightly higher than the ones derived from an earlier configuration[15] because the plume shield focuses the ion beam within the 60-deg half-angle cone. Moreover, the -1-kV bias potential on the plume shield reflects secondary electrons from the collector inside the chamber. Therefore, the emitter current measurement is not influenced by those secondary electrons. It is estimated that those secondary electrons contributed up to a few percent to the earlier measurements.

The ion beam interaction of three In-FEEP thrusters in a triangle configuration was also investigated with beam diagnostics. No interaction, at least up to a distance of 5 cm from the thruster, have been found along the complete thrust range.[15]

The microdroplet angular distribution for a single In-FEEP thruster (extractor diameter 2 mm, emitter–extractor distance 0.6 mm) was investigated using silicon catcher plates.[10] At a distance of 40 mm from the tip, 12 catcher plates (polished Si, 0.3 mm thickness, 1 cm^2 area) were arranged in 15-deg distance along a circular arc with the emitter tip in the center. Droplets deposited on the catcher plates are identified by scanning electron microscopy. The test duration was chosen so that there are sufficient particles in the microscope field of view to yield acceptable counting statistics and that the particle density is not too high so that particles will coagulate or form a continuous In film. Figure 9 shows the normalized angular distribution on a logarithmic scale for an ion current of 100 and 250 μA. The measurement error for angles >40 deg was about 60%, smaller angles yielded values of 20%. Compared to

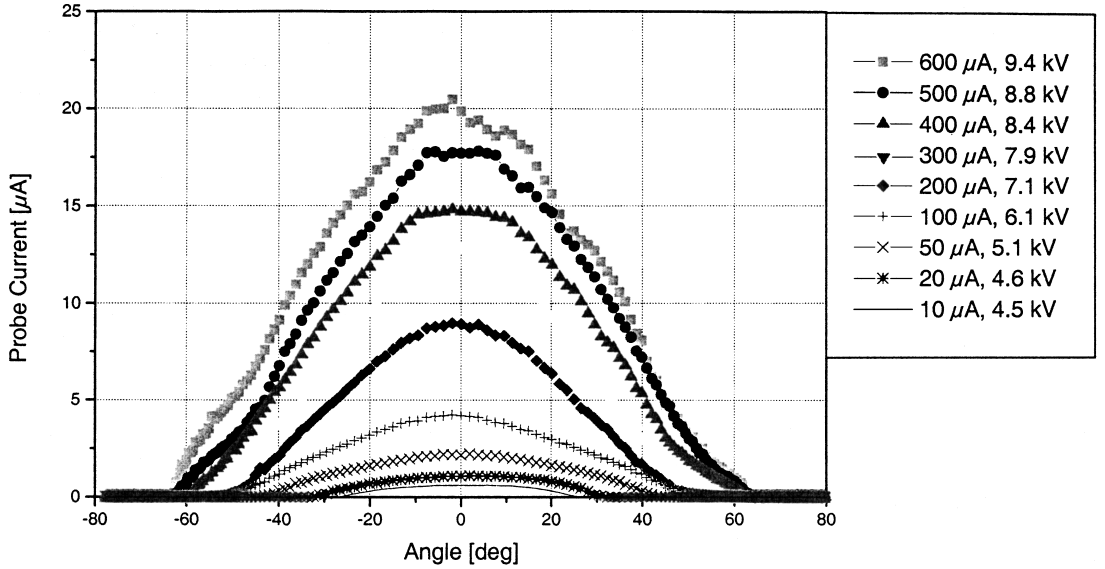

Fig. 6 Ion beam profiles for emitter currents from 10 to 600 μA at $Z = 30$ mm, probe biased at −28 V.

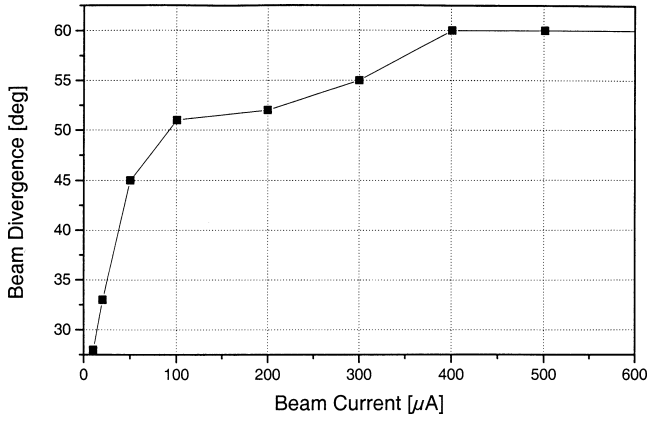

Fig. 7 Total ion beam divergence half-angle for beam currents from 10 to 600 μA.

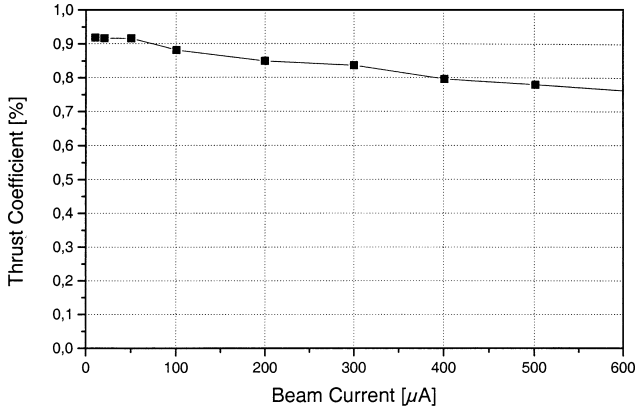

Fig. 8 Computed thrust coefficient factor for beam currents from 10 to 600 μA.

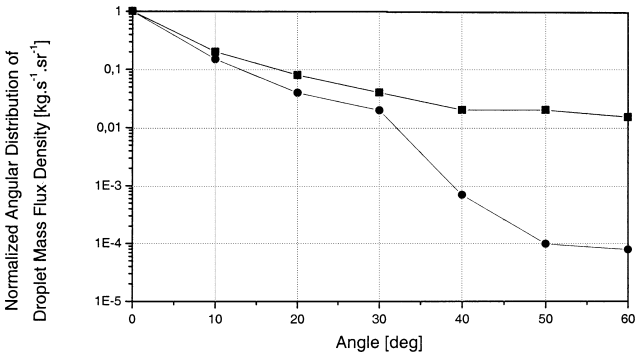

Fig. 9 Normalized angular distribution of microdroplets: ■, ion current 250 μA and ●, ion current 100 μA.

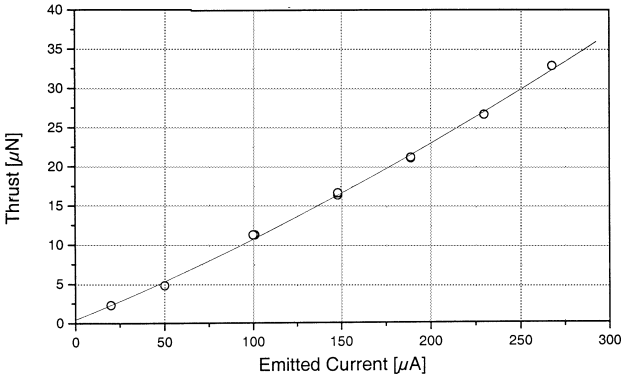

Fig. 10 Direct thrust measurement of capillary In-FEEP thruster at ONERA: ○, thrust in micronewtons and ——, polynomial fit, thrust coefficient factor 80%.

the ion beam distribution, the droplets are much more peaked along the centerline. Also Fig. 9 indicates that the droplet distribution is greatly influenced by space charge.

Direct Thrust Measurements

To validate the thrust equation, direct thrust measurements were carried out at ONERA and NASA Jet Propulsion Laboratory (JPL). The ONERA balance consists of a null-deflection pendulum counterbalanced by magnetic actuators.[13] Figure 10 shows direct thrust measurements using a capillary-type In-FEEP thruster with an extractor hole of 2 mm and an emitter–extractor distance of 0.6 mm (no plume shield). The thrust accuracy in this measurement was about 1 μN over the whole thrust range. The JPL thrust stand[14] consists of a torsion pendulum with submicronewton resolution. Figure 11 shows direct thrust measurements using a needle-type In-FEEP thruster with an extractor hole of 3.5 mm and an emitter–extractor distance of 0.6 mm. The measured thrust coefficients of 77–80% are very well within expectations from previous beam divergence measurements.[15] The lower beam divergence losses in the ONERA

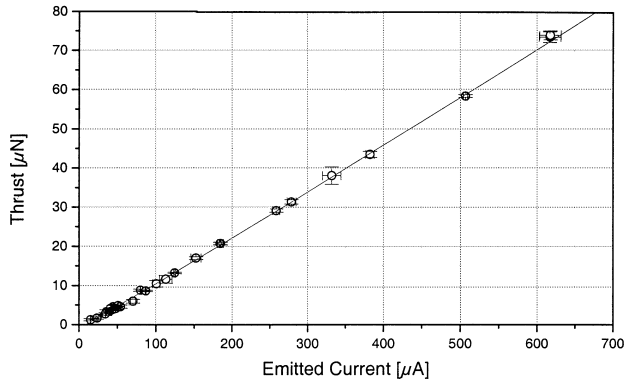

Fig. 11 Direct thrust measurement of needle In-FEEP thruster at NASA JPL: ○, thrust in micronewtons and ——, polynomial fit, thrust coefficient factor 77%.

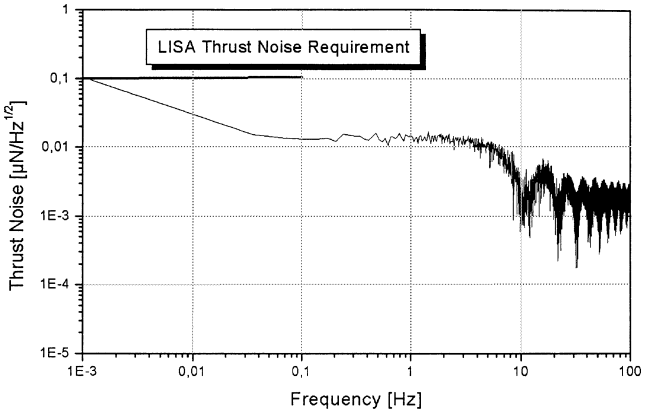

Fig. 12 In-FEEP thrust noise compared to LISA requirement.

experiment are due to the smaller extractor hole, which generates a more narrow ion beam.

Thrust Noise

Because Eq. (1) was experimentally verified, we can use current and voltage signals from the power supply to calculate reliably thrust and also thrust noise. This method is especially useful because direct thrust noise measurements in the micronewton range are a very complicated task. For this purpose, a flight electronic breadboard with a digital feedback loop using current and voltage signals to maintain a certain thrust level, intended to be used for ESA's GOCE mission,[19] was tested together with the In-FEEP thruster to obtain representative thrust noise values. The sampling frequency was set to 1200 Hz followed by a digital fourth-order Butterworth filter with a 150-Hz cutoff frequency. Figure 12 shows the thrust noise derived from a Fourier analysis at a thrust of 8 μN, a typical mean thrust value for missions like LISA. As it can be seen, the thrust noise is below the LISA requirement.

Mass Efficiency

The propellant utilization or mass efficiency η_m is a very important factor determining the propellant reservoir size. It is calculated by weighting the thruster before and after a test to evaluate the total mass loss Δm and the ion current integral,

$$\eta_m = \frac{m_{\text{ion}}}{e} \frac{\int I_E \cdot \mathrm{d}t}{\Delta m} \tag{4}$$

This value expresses the ratio between mass emitted as ions (main thrust constituent) and mass emitted as microdroplets (only little influence on thrust). The lower mass efficiency, the more droplets will be emitted and the larger the propellant reservoir size must be to deliver a certain total impulse. Up to a threshold current (typically 20 μA), mass efficiency is 100%, and no droplets are generated. Higher currents require more indium than is resupplied from the reservoir. This resupply is greatly dominated by the viscosity of the liquid metal and the applied electric field. That causes an interruption of the ion beam and an instability at the tip of the Taylor cone, which results in the emission of microdroplets. Those interruptions are usually in the megahertz frequency range for LMIS.[20,21]

A model has been developed to express mass efficiency as a function of temperature and the current–voltage characteristic of the emitter. This model was verified in a number of tests for both capillary- and needle-type LMIS.[22] As a result, mass efficiency can be expressed by

$$\eta_m \propto \cdot\left(r \cdot I_E \big/ U_E^2\right) \cdot f(\tau) \tag{5}$$

where r is the emitter–extractor distance. The function $f(\tau)$ is higher, the closer the operating temperature τ is to the melting point of indium (156°C). It has been observed that $f(\tau)$ is rather constant up to 200°C. Only above 200°C, $f(\tau)$ drops quickly causing a significant decrease in mass efficiency. Equation (5) relates mass efficiency with the slope of the current–voltage characteristic by $(I \cdot U^{-2})$. A steep I–U characteristic curve (high currents at low voltages) will have a much worse mass efficiency along higher currents than a more flat I–V characteristic (high currents at high voltages) of the same emitter type. Unfortunately, a flat I–U characteristic also means a higher power-to-thrust ratio, which is not a good scaling law for space applications. However, our scaling formalism allows thruster optimization by changing the I–U characteristic, with a tradeoff study regarding the power budget, for a certain mass efficiency.

Figure 13 shows mass efficiency along the emitted current. (The thrust in micronewtons is approximately the current in microamperes divided by 10.) The measurement error below 100 μN was about 5%; higher currents yielded smaller errors of only 1% due to the higher mass loss. By approximating the I–U characteristic with a polynomial function, we can express mass efficiency by

$$\eta_m \propto I^{\beta} \tag{6}$$

This approximation fits the experimental data very well. Once the parameter β is determined for a certain emitter and extractor geometry, it is easy to extrapolate mass efficiency values along the thrust range using this approximation. By knowing mass efficiency, we can also calculate the upper limit of thrust contribution due to droplets. When beam divergence losses are neglected, the complete thrust equation for ions and droplets is given by

$$F = \dot{m} \cdot v \approx I_E \cdot (m/e)_{\text{ion}} \cdot \left[\sqrt{2eU_E(e/m)_{\text{ion}}} + [(1-\eta_m)/\eta_m] \cdot \sqrt{2eU_E(e/m)_{\text{droplet}}}\right] \tag{7}$$

We can then express the ratio of ion-to-droplet thrust and express the lower limit ratio by using the upper limit droplet charge as

$$F_{\text{ion}}/F_{\text{droplet}} = [\eta_m/(1-\eta_m)] \cdot \sqrt{(e/m)_{\text{ion}} \cdot (m/e)_{\text{droplet}}} > 228.8 \cdot \eta_m/(1-\eta_m) \tag{8}$$

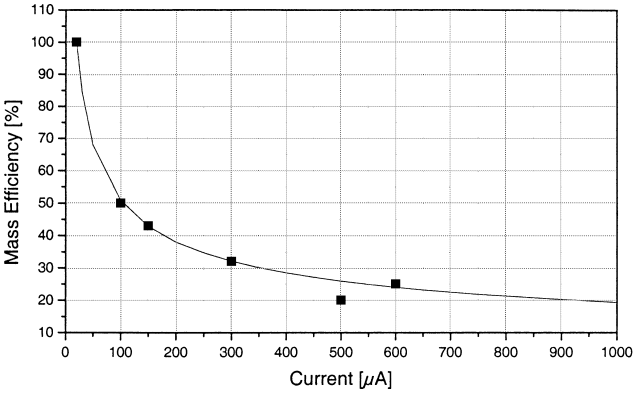

Fig. 13 Mass efficiency vs emitter current: ——, $\eta \propto I^{-0.42}$ and ■, measurements.

This shows that ions are the major contributor to thrust even at very low mass efficiencies (at 1% mass efficiency, $F_{ion}/F_{droplet} > 2.3$). Also as a important result, thrust noise is, therefore, dominated by ions. When a mass efficiency for high thrusts of 20% is considered, the ratio $F_{ion}/F_{droplet} > 57$. This shows that thrust noise due to droplets must be at least one order of magnitude below the one from the beam ions even at maximum thrusts of the In-FEEP thruster.

Operational Characteristics

Figure 14 shows the extractor and plume shield losses for an In-FEEP thruster in the configuration of Fig. 4 (extractor diameter 4 mm, emitter–extractor distance 0.2 mm). This shows that the electrical efficiency of the thruster is always >95%. Using the thrust coefficient values from Fig. 8, we can calculate the thruster performance (excluding the neutralizer) for a typical In-FEEP current–voltage characteristic, ranging from 1 to 64 μN (Fig. 15). Using the mass efficiency measurements from Fig. 13, we can also calculate the thruster's specific impulse (Fig. 16) ranging from 8000 to 1600 s. Figure 16 also shows the power-to-thrust ratio. The heater power for one single In-FEEP thruster is about 0.5 W. A typical high-voltage converter efficiency is 80%. For the total power and mass budgets, the contribution from a neutralizer also has to be taken into account. All neutralizer candidates and a discussion about their suitability for various mission environments and power consumptions are given in Ref. 23. All major performance parameters are summarized in Table 2.

Calculated thrust steps between 0 and 100 μN are shown in Fig. 17. The minimum thrust depends basically on the resolution

Table 2 In-FEEP thruster characteristics

Parameter	Values
Thrust	0.1–100 μN/thruster[a]
Thrust resolution	<0.01 μN
Thrust noise	<0.15 μN[b]
Minimum impulse bit	<5 nN · s
Total impulse	600 N · s/thruster[c]
Specific impulse	1600–8000 s
Singly charged fraction	98%
Electrical efficiency	95%[d]
Total power supply control units power	13 W[e]
Total thruster mass	2.5 kg[e]

[a]Maximum thrust depends on maximum voltage and mass efficiency.
[b]Over a period of 1000 s.
[c]With present 30-g reservoir size; larger sizes possible.
[d]When the current is compared to the emitter with the current in the ion beam (minus extractor and plume shield current losses).
[e]When thermionic neutralizer, heaters, and dc-dc converter losses, are included indium LMIS power-to-thrust ratio alone is about 45–84 W/mN.

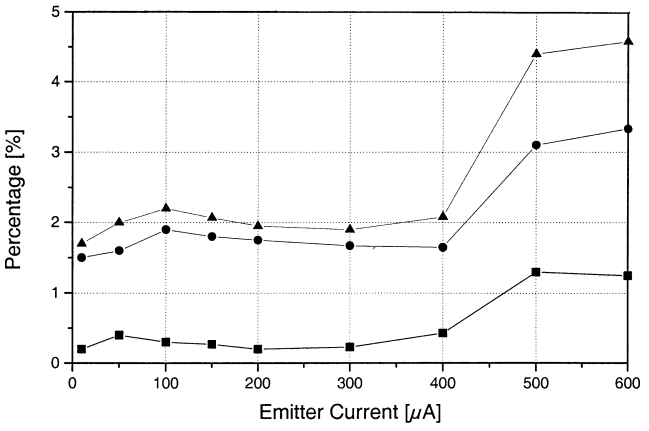

Fig. 14 Extractor and plume shield currents loss for emitter currents from 10 to 600 μA: ■, extractor current loss; ●, plume shield current loss; ▲, total loss.

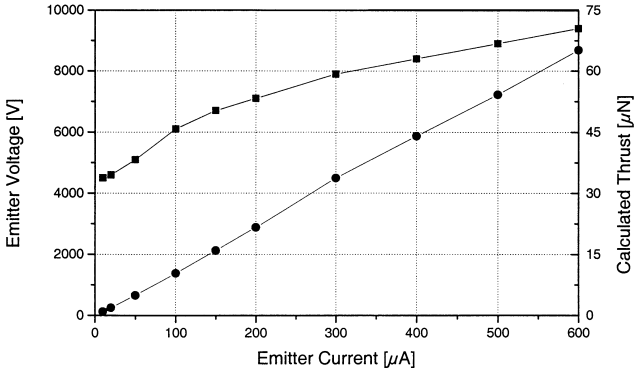

Fig. 15 Typical voltage and calculated thrust for beam currents from 10 to 600 μA: ■, voltage and ●, calculated thrust.

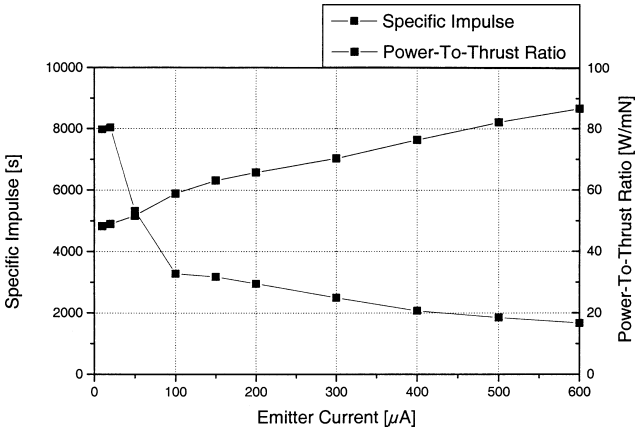

Fig. 16 Specific impulse and power-to-thrust ratio for beam currents from 10 to 600 μA.

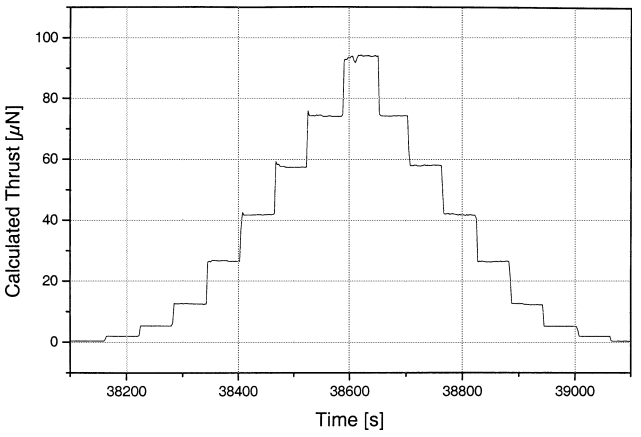

Fig. 17 Calculated thrust steps.

of the high-voltage power supply. Figure 18 shows a stable thrust of 0.4 μN in the current regulation limit of the power supply. We investigated thrust resolution by analyzing a thrust-stabilized signal at 3 μN with a high sampling rate (Fig. 19). This shows that the thrust resolution, calculated from electric measurement, is about 5 nN at this thrust level. Thrust stability at 18 μN is shown in Fig. 20; the standard deviation is 0.72% around the mean value.

No differences in operational parameters such as beam divergence, reproducibility, controllability, and mass efficiency have been found between continuous and pulsed mode operation, at least not in the 1–10 Hz repetition rate range.[2] The In-FEEP thruster can also work in a relatively high background pressure. This was investigated by using a controllable leak in the vacuum chamber. Up to a pressure of 5×10^{-4} mbar, no degradation of operational behavior was found.[2] Higher pressures were prevented due to high-voltage arcing

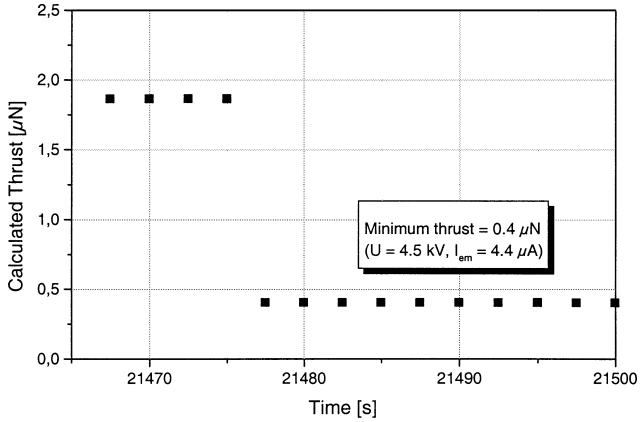

Fig. 18 Calculated minimum thrust limited by power supply resolution.

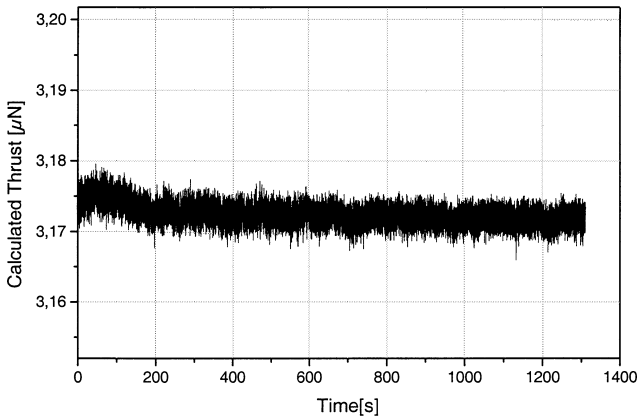

Fig. 19 Calculated thrust resolution at 3 μN.

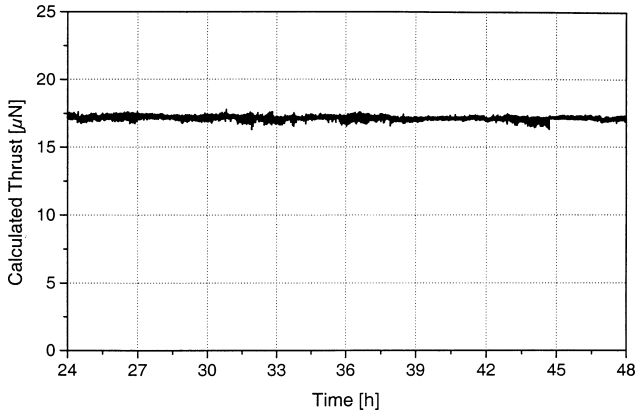

Fig. 20 Calculated thrust stability at 18 μN.

inside the vacuum chamber. Moreover, the In-FEEP thruster can be stored in humid air without performance degradation. This was investigated by storing an indium LMIS in a temperature chamber at 50°C and 90% relative humidity for 5 days (Ref. 24). No performance change was detected other than a slightly higher starting voltage of 200 V (which decreased to its original value after several hours of testing). This avoids spring caps with pyroelements for protection.

Lifetime

To date, 50 indium LMIS launched on various spacecraft have logged more than 2700 h of cumulative operation in space. The current emitted by them corresponds to thrust levels between 2 and 5 μN. Several endurance test campaigns were carried out at thrust levels of 15 μN for 820 h (Ref. 5) (typical thrust level of missions like LISA) and recently with a cluster of two In-FEEP thrusters at thrust profiles ranging from 0 to 33 μN including calibration profiles from 0 to 55 μN for a period of 2000 h. One thruster continued in an ongoing test and already has reached 4000 h (February 2003). No known failure mechanisms have been found after extended firing. All details of this endurance test are given in a separate paper.[25]

Conclusions

A single In-FEEP thruster can operate in a thrust range of 1–100 μN with a resolution better than 0.1 μN. Direct thrust measurements confirm the thrust equation and are consistent with beam profile measurements. Moreover, the thruster can be operated in continuous and pulsed mode and even at high background pressures up to 10^{-4} mbar.

With 50 In-LMIS demonstrating a combined total of 2700 h of space operation and a successful 4000-h endurance test campaign, the In-FEEP thruster has demonstrated significant capability.

Acknowledgments

Part of this work has been carried out under ESTEC Contract 12376/97/NL/PA. All thruster developments were performed at ARC Seibersdorf Research, Austria. The authors would like to thank the Technical Officer Jose González for his continued support. We also acknowledge Michael Fehringer and Friedrich Rüdenauer, who led the early developments of this program, and Nembo Buldrini, who recently joined our group and helped a lot during the endurance test campaign.

References

[1]Ruedenauer, F. G., Fehringer, M., Schmidt, R., and Arends, H., "Operation of Liquid Metal Field Ion Emitters under Microgravity," *ESA Journal*, Vol. 17, No. 2, 1993, p. 147.

[2]Fehringer, M., Ruedenauer, F., and Steiger, W., "Space-Proven Indium Liquid Metal Field Ion Emitters for Ion Microthruster Applications," AIAA Paper 97-3057, July 1997.

[3]Fehringer, M., Ruedenauer, F., and Steiger, W., "Indium Liquid-Metal-Ion-Sources as Micronewton Thrusters," *Proceedings of the 2nd LISA Symposium*, Vol. 456, edited by W. M. Folkner, American Institute of Physics Conf., New York, Dec. 1998.

[4]Genovese, A., Steiger, W., and Tajmar, M., "Indium FEEP Microthruster: Experimental Characterization in the 1–100 μN Range," AIAA Paper 2001-3788, July 2001.

[5]Genovese, A., Tajmar, M., and Steiger, W., "Indium FEEP Endurance Test: Preliminary Results," International Electric Propulsion Conf., Paper IEPC-01-289, Oct. 2001.

[6]Marcuccio, S., Genovese, A., and Andrenucci, M., "Experimental Performance of Field Emission Microthrusters," *Journal of Propulsion and Power*, Vol. 14, No. 5, 1998, pp. 774–781.

[7]Mitterauer, J., "Indium: An Alternative Propellant for FEEP-Thrusters," AIAA Paper 2001-3792, July 2001.

[8]Forbes, R. G., and Ljepojevic, N. N., "Liquid-Metal Ion Source Theory: Electrohydrodynamics and Emitter Shape," *Surface Science*, Vol. 266, No. 1–3, April 1992, pp. 170–175.

[9]Thompson, S. P., and von Engel, A., "Field Emission of Metal Ions and Microparticles," *Journal of Physics D: Applied Physics*, Vol. 15, 1982, pp. 925–931.

[10]Fehringer, M., Ruedenauer, F., and Steiger, W., "WP 2000: Droplet Emission," European Space Research and Technology Center, Technical Note No. 2, ESTEC Contract Report 12376/97/NL/PA, Noordwijk, June 1998.

[11]Tajmar, M., Ruedenauer, F., and Fehringer, M., "Backflow Contamination of Indium Liquid-Metal Ion Emitters (LMIE): Numerical Simulations," International Electric Propulsion Conf., Paper IEPC-99-070, Oct. 1999.

[12]Genovese, A., Buldrini, N., Tajmar, M., and Steiger, W., "2000h Endurance Test on an Indium FEEP Cluster," International Electric Propulsion Conf., Paper IEPC-2003-102, Toulouse, March 2003.

[13]Bonnet, J., Marque, J. P., and Ory, M., "Development of a Thrust Balance in the microNewton Range," 3rd International Conf. on Spacecraft Propulsion, ESA-SP-465, CNES/ESA, Noordwijk, Oct. 2000.

[14]Ziemer, J., "Performance Measurements using a Sub-Micronewton Resolution Thrust Stand," International Electric Propulsion Conf., Paper IEPC-1238, Oct. 2001.

[15]Tajmar, M., Steiger, W., and Genovese, A., "Indium FEEP Thruster Beam Diagnostics, Analysis and Simulation," AIAA Paper 2001-3790, July 2001.

[16]Marrese-Reading, C., Polk, J., Mueller, J., Owens, A., Tajmar, M., Fink, R., and Spindt, C., "In-FEEP Ion Beam Neutralization with Thermionic and Field Emission Cathodes," International Electric Propulsion Conf., Paper IEPC-01-290, Oct. 2001.

[17]Tajmar, M., "Electric Propulsion Plasma Simulations and Influence on Spacecraft Charging," *Journal of Spacecraft and Rockets*, Vol. 39, No. 6, 2002, pp. 886–893.

[18]Tajmar, M., Marhold, K., and Kropatschek, S., "Three-Dimensional In-FEEP Plasmadiagnostics," International Electric Propulsion Conf., Paper IEPC-2003-0163, March 2003.

[19]Johannessen, J. A., and Aguirre-Martinez, M., "Gravity Field and Steady-State Ocean Circulation Mission," *Reports for Mission Selection*, ESA SP-1233, 1999.

[20]Vladimirov, V. V., Badan, V. E., and Gorshkov, V. N., "Microdroplet Emission and Instabilities in Liquid-Metal Ion Sources," *Surface Science*, Vol. 266, 1992, pp. 185–190.

[21]Akhmadaliev, C., Mair, G. R. L., Aidinis, C. J., and Bischoff, L., "Frequency Spectra and Electrohydrodynamic Phenomena in a Liquid Gallium Field-Ion-Emission Source," *Journal of Physics D: Applied Physics*, Vol. 35, Sept. 2002, pp. L91–L93.

[22]Tajmar, M., and Genovese, A., "Experimental Validation of a Mass Efficiency Model for an Indium Liquid Metal Ion Source," *Applied Physics A*, Vol. 76, No. 6, 2003, pp. 1003–1006.

[23]Tajmar, M., "Survey on FEEP Neutralizer Options," AIAA Paper 2002-4243, July 2002.

[24]Steiger, W., Genovese, A., and Tajmar, M., "Micronewton Indium FEEP Thrusters," 3rd International Conference on Spacecraft Propulsion, ESA SP-465, CNES/ESA, Noordwijk, Oct. 2000.

[25]Genovese, A., Tajmar, M., Buldrini, N., and Steiger, W., "Indium Field Emission Electric Propulsion Microthruster Cluster 2000 Hour Endurance Test of Cluster," *Journal of Propulsion and Power*, Vol. 20, No. 2, 2004, pp. 219–227.